Line strengths and self-broadening of pure rotational lines of carbon monoxide measured by terahertz time-domain spectroscopy

Weston Aenchbacher,[1] Mira Naftaly,[2,*] and Richard Dudley[2]

[1]Currently with the Department of Electrical and Computer Engineering, Drexel University, 3141 Chestnut Street, Philadelphia, Pennsylvania 19104, USA

[2]National Physical Laboratory, Hampton Road,Teddington, Middlesex TW11 0LW, UK

*Corresponding author: mira.naftaly@npl.co.uk

Received 23 December 2009; revised 4 March 2010; accepted 2 April 2010; posted 5 April 2010 (Doc. ID 121638); published 26 April 2010

Pure rotational lines of carbon monoxide were observed using terahertz time-domain spectroscopy. Measurements were carried out at elevated pressures of 0.7–5.1 bar. Line intensities and self-broadening parameters of transitions from $J' = 3 \leftarrow 2$ to $J' = 22 \leftarrow 21$ were obtained. Good agreement with the HITRAN database was found. © 2010 Optical Society of America

OCIS codes: 300.6390, 300.6495.

1. Introduction

There is extensive literature on the frequency determination of the pure rotational spectrum of CO and its isotopomers ([1] and references therein). This reflects the significance of CO as a ubiquitous interstellar molecule and an important trace constituent of planetary atmospheres. In addition, owing to its regularly spaced and uncongested line pattern, $^{12}C^{16}O$, in particular, has found utility as a frequency calibration standard in the far infrared [2,3].

A number of high-resolution techniques are available for the measurement of line positions, and they have been used to determine accurately the line frequencies of CO. In particular, terahertz (THz) generation by difference-frequency mixing [2–6], backward-wave oscillator (BWO) sources [7–9], a Fourier transform infrared (FTIR) spectrometer [6], and a grating spectrometer [10] have been utilized. Several of these studies were comprehensive [3,7–10], enabling a direct experimental comparison across the full spectrum of frequencies obtained using different techniques.

In contrast, little work has been done on measuring the line strengths and self-broadening parameters of pure rotational lines of CO. The line strengths of the $J' = 8$ to $J' = 24$ lines were determined by Birk *et al.* [11] using FTIR. Rosasco [12] used coherent anti-Stokes Raman spectroscopy to obtain the self-broadening parameters of the $J' = 1$ to $J' = 35$ lines. In addition, several groups [13–15] measured self-broadening in one or two of the lowest lines using BWO-based spectrometers with a limited tunability range. There are, however, significant differences between the values obtained by [12] and those of [13–15]. ([13–15] investigated different lines, so they are not comparable with each other.) There is, therefore, a paucity of data on the line strengths and self-broadening coefficients of the CO rotational lines.

The determination of line strengths and broadening parameters requires broadband tunability combined with an accurate measurement of absorption coefficients. Terahertz (THz) time-domain spectroscopy (TDS) [16] is, therefore, a particularly suitable technique for such measurements. Although THz TDS offers only a relatively coarse frequency resolution, of the order of 1 GHz, high resolution is not necessary in the measurement of gas line shapes at atmospheric pressure and above. On the other hand,

0003-6935/10/132490-07$15.00/0

THz TDS possesses several important advantages. It is broadband, typically spanning the range of 0.3–3 THz, although some systems achieve higher frequencies of up to 6 THz. The data are acquired in the time domain, from which the spectral information is obtained by applying the Fourier transform. Therefore, the complete spectrum is acquired at once as a single data set. This is particularly important at higher pressures, when the lines partially overlap, and multipeak fits are necessary to determine the individual linewidths and strengths. It is also important that the measurement of transmitted intensity is linear, with a typical dynamic range of several thousand. Moreover, unlike FTIR [11], THz TDS is free of errors associated with instrumental line shape. That is because the resolution and accuracy of the derived spectrum are limited only by the data step interval of the Fourier transform, which is determined by the length of the delay sweep.

THz TDS has indeed been used to study the CO molecule [17]; however, that was a work of limited scope that focused solely on transition frequencies.

In this paper, for the first time, to our knowledge, we use THz TDS to perform a detailed study of the line strengths and self-broadening parameters of a gas molecule. We apply the technique to the pure rotational transitions of the CO molecule for the lines $J' = 3$ to $J' = 22$. In the area where few experimental results are documented, the obtained data may serve to support the HITRAN database.

2. Experimental

The TDS system is described in detail elsewhere [18,19] and is a commonly used type employing a biased photoconductive emitter and electro-optic detection. The THz beam path is enclosed in an airtight box that is purged with dry air in order to eliminate water absorption lines from the measured spectra. Since the gas absorption spectrum is calculated with respect to the reference spectrum (i.e., gas cell filled with dry N_2), the water vapor in the beam path must be eliminated only to the level where water absorption lines disappear from the measured gas spectrum. The gas cell (see below) is positioned in the collimated arm of the THz beam path.

The gas cell was an aluminum cylinder 300 mm in length, with a 100 mm inner diameter, equipped with a Bourdon dial pressure gauge. The two end windows were polytetrafluoroethylene (PTFE) and were 5 mm thick. PTFE was chosen due to its high transparency at THz frequencies [20]. Measurements were carried out at the ambient temperature of 297 K.

Unlike previous studies of the CO far-infrared spectrum, which used pressures of a few millibars or less, in the present work measurements were done at high pressures varying between 0.7 and 5 bar. This allowed comparisons to be made between linewidth and self-broadening data acquired in different pressure regimes.

Carbon monoxide gas was supplied by BOC with a purity of >99.5% $k = 2$. The isotopomer mix was that of natural abundance.

3. Data Acquisition and Analysis

The absorption peaks of transitions from $J' = 3$ to $J' = 21$ were studied. This range was determined by the available measurement bandwidth and the variable dynamic range of the system [17].

The time-domain data sets were acquired by sweeping the delay over a distance of 120 mm, i.e., scanning over a time delay of 800 ps. The calculated frequency-domain spectra, therefore, had a data interval of 1.25 GHz.

In the simplest approach, the frequency resolution of a TDS system can be taken as the step interval of the FFT data set, given by $c/2L$, where L is the length of the delay sweep. In principle, given an arbitrarily long delay line, the resolution of a TDS is ultimately limited by the repetition rate of the pump laser, which is typically around 80 MHz for femtosecond lasers. However, in practice, the achievable resolution is much lower and is set by the noise floor of

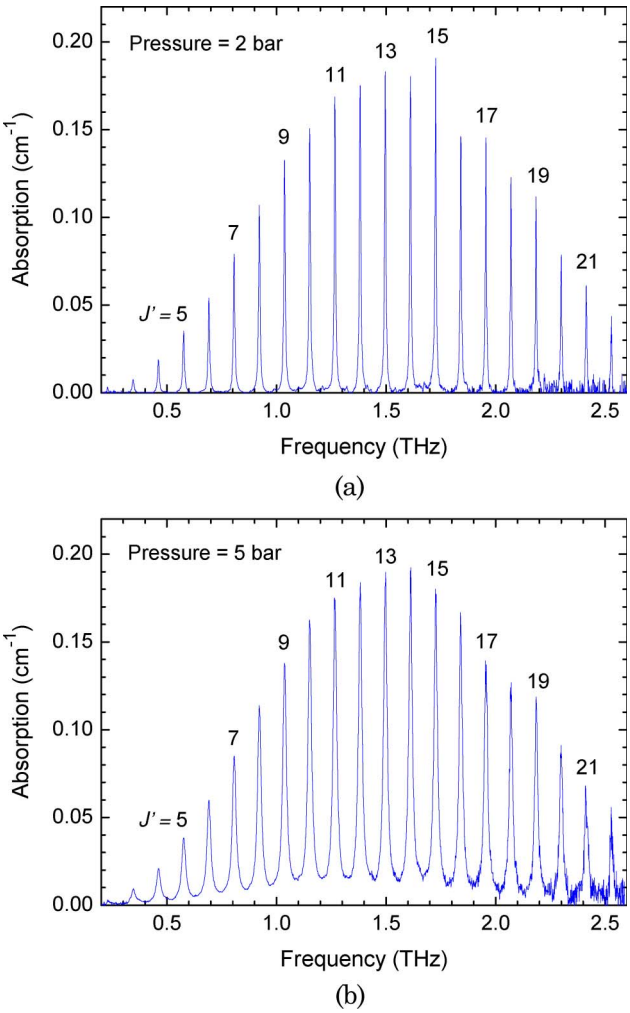

Fig. 1. (Color online) CO absorption spectra at (a) 2 and (b) 5 bar measured by THz TDS, showing line broadening.

the system [21]. In common experimental practice, the maximum sweep length is limited by the delay where the THz signal remains at least a factor of 2 above the noise floor (the RMS noise in the absence of signal) of the detector. However, the center frequency of symmetrical peaks can be determined with considerably higher accuracy than the step interval of the spectral data (see Section 4).

The frequency-dependent absorption coefficient $\alpha(\nu)$ was calculated from the Beer–Lambert equation:

$$\alpha(\nu) = -2\ln[E(\nu)/E_0(\nu)]/d, \quad (1)$$

where ν is the THz frequency, E is the field amplitude of the THz beam transmitted through the gas cell, E_0 is the field amplitude of the reference THz beam, d is the path length through the gas in the cell, and the factor 2 is required because TDS measures field amplitude rather than intensity.

Data analysis, including FFT, calculation of absorption spectra, spectral profile fittings, and linear least-squares calculations, was accomplished using OriginPro 8 software, which provides built-in routines for such calculations. The FFT amplitude spectrum was calculated using the rectangular windowing function (Fig. 1). Absorption peak profiles were fitted using the Lorentzian function (Figs. 2 and 3). The Lorentzian was chosen in preference to Voigt because the Doppler (Gaussian) component of broadening (~0.5 MHz) is well below the frequency resolution of the THz TDS system and, at the pressures used in the experiments, is negligible compared with collisional self-broadening (Lorentzian) [12–14].

As seen in Figs. 2 and 3, there was no evidence of line mixing leading to non-Lorentzian line shapes and line narrowing [22], even at the pressure of 5 bar. We found no observations reported in the literature of line mixing in pure rotational lines; although the effect has been observed in rotational–vibrational

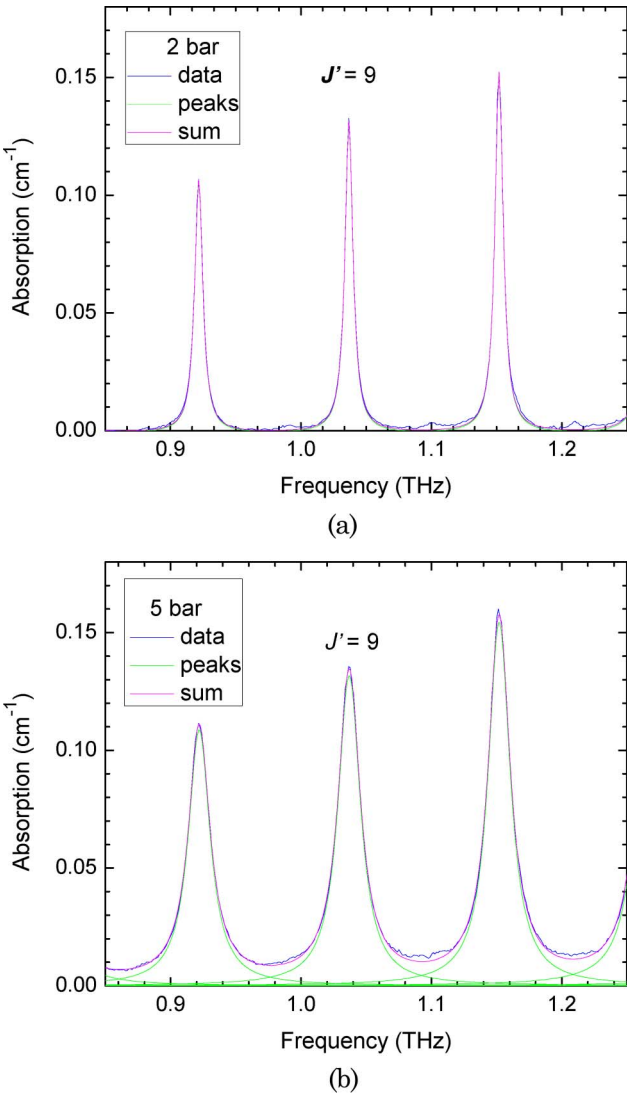

Fig. 2. (Color online) Section of the CO absorption spectrum at (a) 2 and (b) 5 bar showing a Lorentzian multipeak fit.

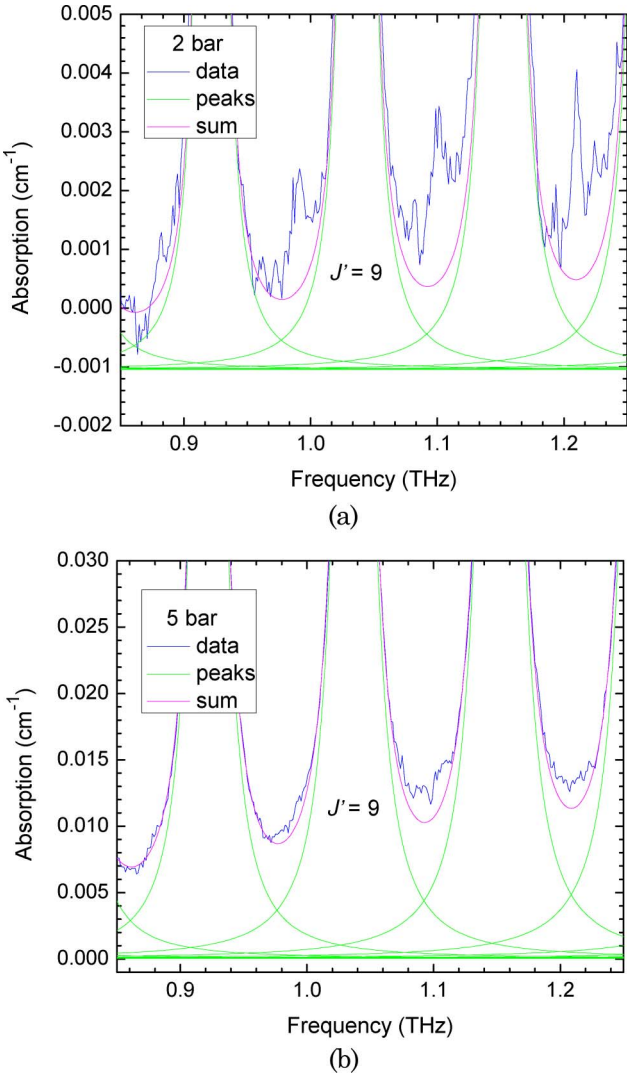

Fig. 3. (Color online) Expanded section of the CO absorption spectrum at (a) 2 and (b) 5 bar showing a Lorentzian multipeak fit. The multipeak fit (upper smooth curve) takes into account the overlap of the wings of the individual peaks (lower curve).

Table 1. Line Intensities and Self-Broadening Parameters of CO Obtained in this Work and Their HITRAN Values

	Line Intensities ($(cm^{-1}/molecule.cm^{-2}) \times 10^{-22}$)			Self-Broadening (GHz/atm)		
$J' \leftarrow J''$	Measured	Standard Deviation	HITRAN	Measured	Standard Deviation	HITRAN
3←2	0.89	0.02	0.821 ± 0.008	2.33	0.10	2.37 ± 0.08
4←3	1.81	0.02	1.82 ± 0.02	2.23	0.02	2.25 ± 0.08
5←4	3.28	0.02	3.262 ± 0.03	2.14	0.01	2.19 ± 0.08
6←5	5.05	0.05	5.075 ± 0.05	2.07	0.02	2.10 ± 0.07
7←6	6.76	0.06	7.117 ± 0.07	2.02	0.02	2.07 ± 0.07
8←7	9.00	0.07	9.206 ± 0.09	1.96	0.02	2.01 ± 0.07
9←8	11.09	0.09	11.14 ± 0.11	1.96	0.01	1.98 ± 0.07
10←9	12.99	0.09	12.75 ± 0.12	1.96	0.01	1.92 ± 0.07
11←10	13.77	0.10	13.88 ± 0.14	1.89	0.01	1.89 ± 0.07
12←11	14.36	0.10	14.47 ± 0.14	1.83	0.01	1.86 ± 0.07
13←12	14.35	0.10	14.49 ± 0.14	1.83	0.01	1.83 ± 0.06
14←13	14.07	0.10	13.99 ± 0.14	1.81	0.01	1.83 ± 0.06
15←14	13.52	0.09	13.04 ± 0.13	1.89	0.01	1.80 ± 0.06
16←15	11.78	0.09	11.77 ± 0.12	1.80	0.01	1.77 ± 0.06
17←16	10.11	0.08	10.31 ± 0.10	1.72	0.01	1.74 ± 0.06
18←17	8.32	0.08	8.761 ± 0.09	1.61	0.01	1.71 ± 0.06
19←18	7.28	0.07	7.239 ± 0.07	1.66	0.02	1.68 ± 0.06
20←19	5.51	0.07	5.82 ± 0.05	1.54	0.02	1.65 ± 0.06
21←20	4.30	0.07	4.556 ± 0.05	1.40	0.03	1.62 ± 0.06
22←21	2.87	0.06	3.476 ± 0.03	1.40	0.04	1.59 ± 0.06

lines of He-broadened CO at pressures above 5 bar [22], it was not seen in other similar measurements [23,24].

It was found that multipeak fittings whereby all the peaks in the spectrum were fitted simultaneously produced better fits with lower residuals than separate single-peak fits (Figs. 2 and 3). This was especially the case at higher pressures, where the overlap between adjacent peaks became increasingly significant. Although the frequency interval of the spectral data was 1.25 GHz, the effective frequency resolution of peak position determination varied between 0.01 and 0.1 GHz, as given by the uncertainty in the fitted center frequency.

Although the measured absorption lies everywhere above zero, a small baseline offset is seen in the fitted baseline in Fig. 3, which is negative at 2 bar and positive at 5 bar. This offset arises from the peak-fitting procedure that allowed the baseline to be a fitting parameter, rather than fixing it at zero, in order to improve the quality of the fit (reduce the sum of residuals). The resulting error in the peak amplitude was $<0.5\%$, and was taken into account in estimating the uncertainty in the calculated line strength.

Both the line strengths and the self-broadening parameters for each peak were obtained by plotting the values as a function of pressure and calculating a linear least-squares fit (Figs. 5 and 6). The peak center frequencies were also plotted against pressure, in order to reveal any evidence of a pressure shift (Fig. 4).

The THz TDS system yields amplitude measurements that are linear, with an uncertainty better than 0.1% [18]. The noise in the system will produce random errors that are reflected in the uncertainties of the peak-fit parameters. The largest systematic uncertainties in the obtained line parameters arise from factors associated with the gas cell. The gas pressure in the cell was monitored by a Bourdon dial gauge, which had an uncertainty of 0.05 bar in determining the dial reading (due to parallax and needle thickness). The dial gauge scale was verified using a National Physical Laboratory calibrated pressure transducer (DH Instruments RPM4). The errors in the pressure readings were random and are incorporated in the error values yielded by the linear least-squares calculations of line intensities and widths. Measurements were carried out at the ambient temperature of 297 ± 1 K. The temperature variations result in 0.3% variations in the calculated line intensities; these are also incorporated in the errors of the least-squares fits. The length of the gas cell was 300 ± 1 mm. The uncertainty in the optical path through the gas gave rise to an independent

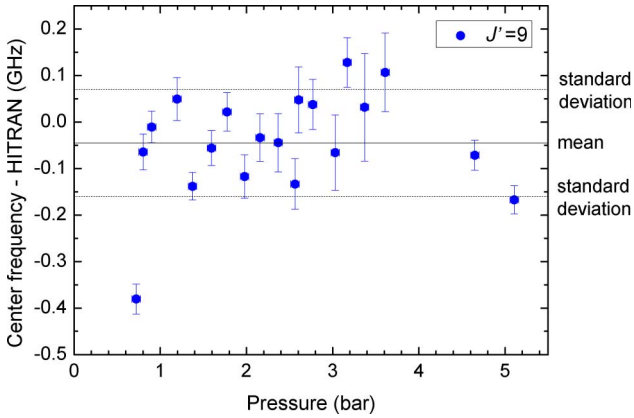

Fig. 4. (Color online) Difference between the measured peak frequencies of the $J' = 9 \leftarrow 8$ transition of CO and its HITRAN value at different gas pressures (the error bars represent standard deviation).

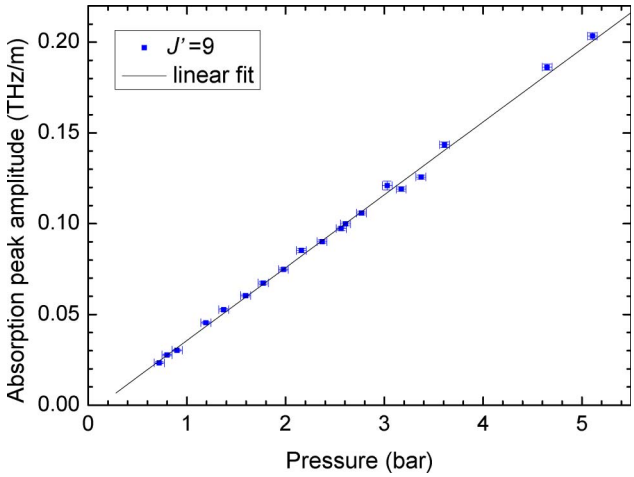

Fig. 5. (Color online) Absorption peak amplitude of the $J' = 9 \leftarrow 8$ transition of CO as a function of pressure. Peak amplitudes are obtained from Lorentzian peak fits (the error bars represent standard deviation).

additional systematic error in the calculated line intensities of 0.3%.

4. Results

Figure 1 plots the CO spectrum obtained by THz TDS at the pressure of 2.0 bar. It is seen that the line profiles are clearly defined and that the noise is insignificant, except close to the baseline. Figures 2 and 3 show a section of the spectrum together with the fitted Lorentzian peaks.

Figures 4–6 present an example of data analysis for the peak $J' = 9$. The variation of the line position with pressure is examined in Fig. 4, which plots the difference between the center frequency and the value cited by the HITRAN database [1]. The frequency error bars are the uncertainties of the least-squares peak fitting. It is notable that the frequency uncertainties and deviations from the HITRAN value that are achieved by peak fitting are, for the most part, an

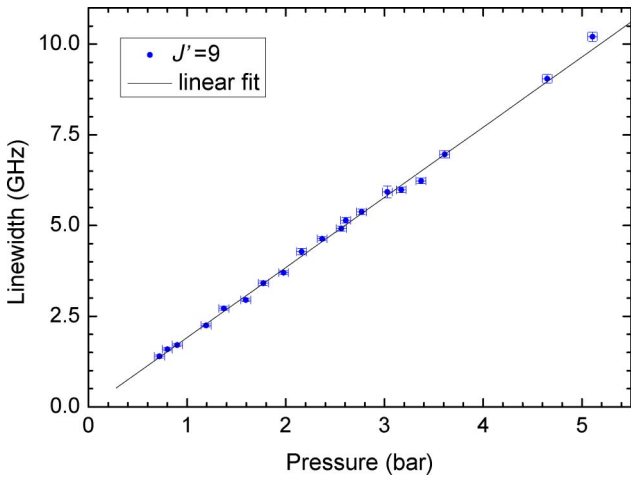

Fig. 6. (Color online) Absorption linewidth of the $J' = 9 \leftarrow 8$ transition of CO as a function of pressure. Linewidths are obtained from Lorentzian peak fits (the error bars represent standard deviation).

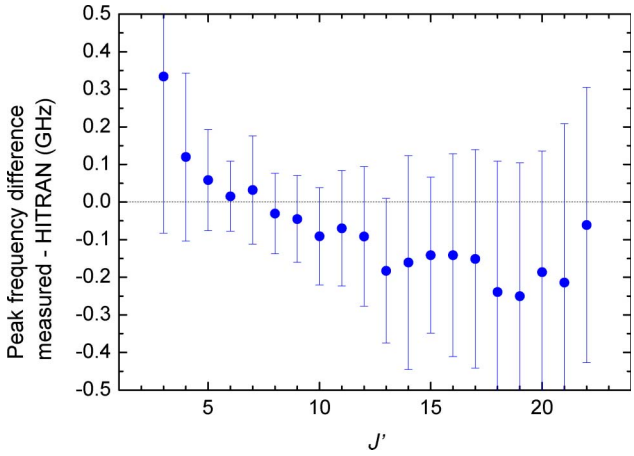

Fig. 7. (Color online) Differences between the measured peak frequencies of CO lines and their HITRAN values (the error bars represent standard deviation).

order of magnitude smaller than the spectral data interval (1.25 GHz). Even the point of greatest deviation (at −0.4 GHz) differs from the expected HITRAN value by less than a third of the data interval. As expected, no pressure-dependent frequency shift is observed in the data. This was also the case for all other observed lines.

The intensity and the self-broadening parameter of the $J' = 9$ line are obtained as shown in Figs. 5 and 6, where the absorption peak amplitude and width, respectively, are plotted as a function of pressure together with the least-squares linear fits. The slopes of the respective fits give the intensity and self-broadening of the line. As noted in Section 3, the absorption peak amplitudes and widths are obtained from Lorentzian fits to the measured spectra. The peak amplitude values A are, therefore, related to the measured absorption coefficients α and linewidths w as $A = \pi\alpha w/2$.

The frequency measurement of the THz TDS is verified by comparing the obtained frequencies for all lines with the HITRAN database [1]. Figure 7

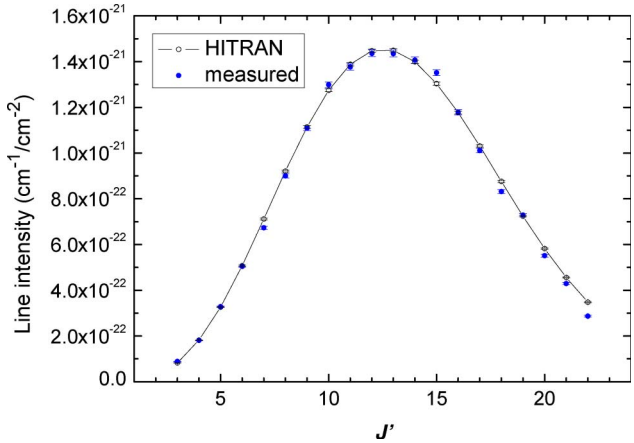

Fig. 8. (Color online) Line intensities of CO lines obtained in this work together with HITRAN values (the error bars represent standard deviation).

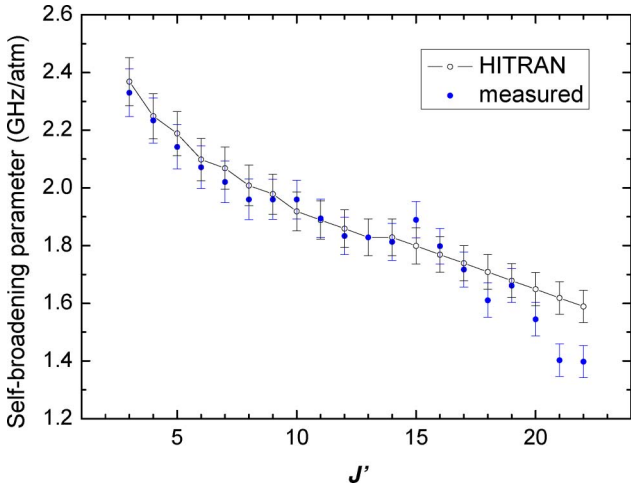

Fig. 9. (Color online) Self-broadening parameters of CO lines obtained in this work together with HITRAN values (the error bars represent standard deviation).

plots for each line the difference between the measured center frequency averaged over all pressures and the HITRAN value. As in Fig. 4, it is seen that the error in the determination of the center frequency is considerably smaller than the step interval of the spectral data. The errors are largest at the edges of the spectrum, where the absorption lines are weaker and the dynamic range of the THz TDS is reduced [18].

Figures 8 and 9 and Table 1 present the line intensities and self-broadening parameters obtained in this work together with the values cited by HITRAN [1]. A good agreement is evident. The uncertainties of THz TDS measurements of these quantities are comparable with those achieved by other techniques [11,12] and those quoted by HITRAN [1]. However, it must be noted that the uncertainties of THz TDS increase greatly at the edges of its bandwidth (below 0.4 THz and above 2.2 THz), where the signal-to-noise ratio of the system is reduced.

5. Conclusion

THz TDS was used to measure the line intensities and self-broadening parameters of pure rotational transitions of CO. The obtained values are in good agreement with the HITRAN database. The database is a compilation of available experimental data, aided where necessary by theoretical model calculations. Owing to the difficulties of far-infrared measurements, little experimental work has been carried out on determining the line strengths and broadening parameters of gas molecules in the far infrared. The presented results offer much needed measurements on the CO molecule. The ease and convenience of THz TDS, together with its broadband nature and high signal-to-noise ratio, make it a demonstrably useful technique for gas spectroscopy.

Financial support for this work was provided by the National Measurement Office, an Executive Agency of the Department for Business, Innovation, and Skills. W. Aenchbacher was on the MSc program of the University of St. Andrews.

References

1. L. S. Rothman, I. E. Gordon, A. Barbe, D. C. Benner, P. F. Bernath, M. Birk, V. Boudon, L. R. Brown, A. Campargue, J.-P. Champion, K. Chance, L. H. Coudert, V. Dana, V. M. Devi, S. Fally, J.-M. Flaud, R. R. Gamache, A. Goldman, D. Jacquemart, I. Kleiner, N. Lacome, W. J. Lafferty, J.-Y. Mandin, S. T. Massie, S. N. Mikhailenko, C. E. Miller, N. Moazzen-Ahmadi, O. V. Naumenko, A. V. Nikitin, J. Orphal, V. I. Perevalov, A. Perrin, A. Predoi-Cross, C. P. Rinsland, M. Rotger, M. Šimečková, M. A. H. Smith, K. Sung, S. A. Tashkun, J. Tennyson, R. A. Toth, A. C. Vandaele, and J. Vander Auwera, "The HITRAN 2008 molecular spectroscopic database," J. Quant. Spectrosc. Radiat. Transfer **110**, 533–572 (2009).
2. I. G. Nolt, J. V. Radostitz, G. Dilonardo, K. M. Evenson, A. Jennings, R. Leopold, M. D. Vanek, L. R. Zink, A. Hinz, and K. V. Chance, "Accurate rotational constants of CO, HCI, and HF: spectral standards for the 0.3- to 6-THz (10- to 200- cm^{-1}) region," J. Mol. Spectrosc. **125**, 274–287 (1987).
3. T. D. Varberg and K. M. Evenson, "Laser spectroscopy Of carbon monoxide: a frequency reference for the far Infrared," IEEE Trans. Instrum. Meas. **42**, 412–414 (1993).
4. S. Matsuura, M. Tani, H. Abe, K. Sakai, H. Ozeki, and S. Saito, "High-resolution terahertz spectroscopy by a compact radiation source based on photomixing with diode lasers in a photoconductive antenna," J. Mol. Spectrosc. **187**, 97–101 (1998).
5. H. M. Pickett, P. Chen, J. C. Pearson, S. Matsuura, and G. A. Blake, "Construction of a three-diode-laser terahertz difference-frequency synthesizer," 25 Nov. 1999, http://trs-new.jpl.nasa.gov/dspace/bitstream/2014/18450/1/99-1932.pdf.
6. H. Sun, Y. J. Ding, and Y. B. Zotova, "Differentiation Of CO isotopic variants by frequency tuning a terahertz source," Appl. Opt. **46**, 3976–3980 (2007).
7. G. Winnewisser, S. P. Belov, Th. Klaus, and R. Schieder, "Sub-Doppler measurements on the rotational transitions of carbon monoxide," J. Mol. Spectrosc. **184**, 468–472 (1997).
8. G. Klapper, F. Lewen, R. Gendriesch, S. P. Belov, and G. Winnewisser, "Sub-Doppler measurements of the rotational spectrum of $^{13}C^{16}O$," J. Mol. Spectrosc. **201**, 124–127 (2000).
9. G. Klapper, L. Surin, F. Lewen, H. S. P. Muller, I. Pak, and G. Winnewisser, "Laboratory precision measurements of the rotational spectrum of $^{12}C^{17}O$ and $^{13}C^{17}O$," Astrophys. J. **582**, 262–268 (2003).
10. K. N. Rao, R. V. de Vore, and E. K. Plyler, "Wavelength calibrations in the far infrared (30 to 1000 microns)," J. Res. Natl. Bur. Stand. Sect. A **67**, 351–358 (1963).
11. M. Birk, D. Hausamann, G. Wagner, and J. W. Johns, "Determination of line strengths by Fourier-transform spectroscopy," Appl. Opt. **35**, 2971–2985 (1996).
12. G. J. Rosasco, "Fundamental molecular data to support CARS diagnostics of temperature, pressure, and species concentration," U. S. Army Research Office, Proposal 23356-Ch (U. S. National Institute of Standards and Technology, August 1989).
13. S. P. Belov, M. Yu. Tretyakov, and R. D. Suenram, "Improved laboratory rest frequency measurements and pressure shift and broadening parameters for the $J = 2 \leftarrow 1$ and $J = 3 \leftarrow 2$ rotational transitions of CO," Astrophys. J. **393**, 848–851 (1992).
14. H. Mader, A. Guarnieri, J. Doose, N. Nissen, V. N. Markov, A. M. Shtanyuk, A. F. Adrianov, V. N. Shanin, and A. F. Krupnov, "Comparative studies of $J' \leftarrow J = 1 \leftarrow 0$ CO line parameters in frequency and time domains," J. Mol. Spectrosc. **180**, 183–187 (1996).
15. V. N. Markov, G. Yu. Golubiatnikov, V. A. Savin, D. A. Sergeev, A. Guarnieri, and H. Mader, "Line broadening and shifting

studies of the $J = 5 \leftarrow 4$ transition of carbon monoxide perturbed by CO, N_2 and O_2," J. Mol. Spectrosc. **212**, 1–5 (2002).
16. P. Y. Han and X.-C. Zhang, "Free-space coherent broadband terahertz time-domain spectroscopy," Meas. Sci. Technol. **12**, 1747–1756 (2001).
17. Y. Hu, X. Wang, L. Guo, and C. Zhang, "Terahertz time-domain spectroscopic study of carbon monoxide," Spectrosc. Spectral Anal. **26**, 1008–1011 (2006).
18. M. Naftaly and R. Dudley, "Methodologies for determining the dynamic ranges and signal-to-noise ratios of terahertz time-domain spectrometers," Opt. Lett. **34**, 1213–1215 (2009).
19. M. Naftaly and R. Dudley, "Linearity calibration of amplitude and power measurements in terahertz systems and detectors," Opt. Lett. **34**, 674–676 (2009).
20. Y.-S. Jin, G.-J. Kim, and S.-G. Jeon, "Terahertz dielectric properties of polymers," J. Korean Phys. Soc. **49**, 513–517 (2006).
21. S. Mickan, J. Xu, J. Munch, X.-C. Zhang, and D. Abbott, "The limit of spectral resolution in THz time-domain spectroscopy," Proc. SPIE **5277**, 55–64 (2004)..
22. F. Thibault, J. Boissoles, R. Le Doucen, and C. Boulet, "Measurement of line interference parameters for the CO-He system," Europhys. Lett. **12**, 319–323 (1990).
23. V. M. Devi, D. C. Benner, M. A. H. Smith, C. P. Rinsland, and A. W. Mantz, "Determination of self- and H_2-broadening and shift coefficients in the 2-0 band of $^{12}C^{16}O$ using a multispectrum fitting procedure," J. Quant. Spectrosc. Radiat. Transfer **75**, 455–471 (2002).
24. A. W. Mantz, V. M. Devi, D. C. Benner, M. A. H. Smith, A. Predoi-Cross, and M. Dulick, "A multispectrum analysis of widths and shifts in the 2010–2260 cm^{-1} region of $^{12}C^{16}O$ broadened by helium at temperatures between 80 and 297 K," J. Mol. Struct. **742**, 99–110 (2005).